





Determination of the Rupture Risk of Cerebral Aneurysms via the Application of a Narrow Neural Network Classifier

Meltem Yavuz Çelikdemir^{1*}, Ayhan Akbal²

¹Tatvan Vocational School, Bitlis Eren University, Bitlis 13100, Türkiye

²Department of Electrical and Electronics Engineering, Fırat University, Elazığ 23100, Türkiye

Corresponding Author Email: mycelikdemir@beu.edu.tr

Copyright: ©2025 The authors. This article is published by IETA and is licensed under the CC BY 4.0 license (<http://creativecommons.org/licenses/by/4.0/>).

<https://doi.org/10.18280/ts.420224>

ABSTRACT

Received: 29 May 2024

Revised: 12 December 2024

Accepted: 12 March 2025

Available online: 30 April 2025

Keywords:

ruptur, machine learning, subarachnoid hemorrhage

Determining the risk of rupture in cases of unruptured cerebral aneurysms is critical for the treatment process. Certain morphological and hemodynamic parameters have been investigated to discover their effects on the risk of rupture. The present study aimed to determine the rupture risk rate of unruptured cerebral aneurysms by examining age, sex, location, width, length, type, and comorbidity parameters. For this purpose, the data were categorized using different classifiers with supervised machine learning for 220 patients diagnosed with cerebral aneurysms between the years 2011 and 2022. Of the patients, 127 had unruptured aneurysms, while 93 had experienced ruptured aneurysms. The training was conducted by applying the Narrow Neural Network classifier algorithm. This algorithm was preferred for its capability to deliver satisfactory performance in learning and classification tasks using limited datasets. Based on the results of the analysis, the rupture risk for the training network was classified with 75% accuracy, and the validation accuracy in the testing process was calculated with 81.8% success. The close values of the validation rates in the training and test scenarios indicate the high level of success at which this study was conducted. Although no ruptures were noted in the radiology reports for three of the patients, the machine learning classification algorithm predicted that ruptures would occur in these patients over time. Upon examination of the disease history of these patients, which included the results recorded in radiology reports completed at later dates, the aneurysms of all three were observed to have ruptured. This model revealed with great accuracy that for ruptured cerebral aneurysms, middle cerebral artery location and a size of 2-10 mm constitute the primary morphological factors, while heart and hypertension comorbidities represent the major hemodynamic parameters. These findings highlight the potential of the NNN algorithm model to evaluate aneurysms of all sizes with high accuracy, without the need for exclusion criteria. This is the first known study to incorporate such a diverse range of comorbidity parameters, along with detailed information on the aneurysm's laterality (right-left) and segment location, in determining rupture status.

1. INTRODUCTION

With recent advances in technology, the number of fields suitable for the application of machine learning has gradually increased. This topic has frequently been addressed by researchers, especially in the field of medicine for the diagnosis of diseases [1-4]. Two main categories of machine learning have been studied in the literature: supervised and unsupervised learning methods. In supervised learning, the data set is divided into training and testing sets. The program is derived from the training set and an algorithm is developed, the accuracy of which is then evaluated using the test set. The purpose of the algorithm is to employ the developed algorithm to predict the outcome of new data [5]. Unsupervised learning aims to find the desired hidden structure in the data set without the use of accuracy data to predict the results [6].

Brain aneurysms are protrusion-shaped enlargements of cerebral arteries [7]. Although unruptured aneurysms have

been reported to occur in 3% of the population, recent studies have projected that the actual rate may be as high as 11% [8]. This condition affects the population and poses a potential risk of rupture [9]. Rupture of brain aneurysms causes subarachnoid hemorrhage, an adverse outcome known as hemorrhagic stroke [7]. Researchers have determined that small-sized intracranial aneurysms constitute 35-47% of ruptured aneurysms [8, 10, 11]. As there is currently no consensus on whether to intervene in an unruptured aneurysm, evaluating the risk of rupture constitutes a critically important parameter for disease treatment and follow-up [10-13]. In unruptured aneurysms, the risk of rupture can be prevented by microsurgery or endovascular treatment [13, 14]. In recent years, numerous studies in the literature have emphasized that the detection of intracranial aneurysms can be achieved with high accuracy using machine learning algorithms [1, 11, 15, 16]. The effect of hemodynamic factors on the rupture of Middle Cerebral Artery (MCA) aneurysms under different

operating conditions has been investigated. The effects of mean wall shear stress, velocity in pressure distribution, and blood viscosity were examined. As a result, the average wall shear stress was observed to increase proportionally with the blood flow rate, and exceeding a value of 0.6 increased the risk of aneurysm rupture. In addition, another study demonstrated that an increase in blood velocity increases the risk of rupture in aneurysms [17]. In a study based on automatic detection of brain aneurysms, training was conducted by cross-validating TOF-MRA image data containing information on 284 patients using a deep learning model. 3D U-Net learning was performed with a total of 198 aneurysms in the data set consisting of 157 images with aneurysms and 127 without. Aneurysm location, such as ACA, MCA, and ICA (Anterior, Middle, and Interior Cerebral Artery, respectively), size (≤ 7 mm, 7-9 mm, 10-19 mm, and ≥ 20 mm), and age of the patient were also included in the study. The model was trained and evaluated on a GeForce RTX 2080 Ti GPU (11GB GDDR6) with TensorFlow 2.4.0. Performance metrics for the best model achieved a false positive rate of 0.8 per patient and a sensitivity of 83%. In addition, the PHASES scores for aneurysms were calculated and categorized as low, medium, or high-risk groups. Low-risk aneurysms were determined to require monitoring, while medium and high-risk aneurysms require treatment. The size and location of the aneurysm were observed not to present significant effects in terms of sensitivity to rupture [18]. For the PHASES score calculations, age, hypertension, history of subarachnoid hemorrhage, aneurysm size, and site predictors were evaluated in 230 patients and compared with populations from North America and Europe (excluding Finland). The risk of aneurysm rupture was found to be 3.6 times higher in Finnish people and 2.8

times higher in Japanese people [19]. In addition, prediction of sugarcane disease and early diagnosis of Alzheimer's disease can be made by using Convolutional Neural Network (CNN) models [20, 21]. In a study, the efficacy of deep learning methods was evaluated in the early, intermediate and advanced stages of Diabetic Retinopathy diagnosis using fundus images [22]. Additionally, an effective image segmentation approach and classification techniques have been devised for the detection and classification of Alzheimer's and Parkinson's disease [23].

Many hemodynamic parameters have been considered in determining the rupture risk status of aneurysms. However, separate evaluations have not been performed for each of these risk factors. In terms of morphological features, they are associated with the rupture risk status of the aneurysm, but the extent of the effect has yet to be clarified [24, 25], constituting a significant gap in the literature. Another major deficiency in the literature is the limited number of studies examining comorbidities. In order to address this issue, the present study examined morphological and hemodynamic characteristics and their relationships in 220 patients with aneurysms aged 22-94 years to determine the rupture risk of cerebral aneurysms. These relationships were evaluated using machine learning classification algorithms and then tested with the data of 33 external patients to assess the classifications. An additional gap in the literature is the partial lack of information regarding aneurysm location. In this study, this deficiency was eliminated by including right-left and segment (M1, M2, M3, M4) information for each aneurysm. Studies in the literature examining morphological and hemodynamic features for identifying and automatically detecting rupture risk by means of machine learning methodologies are shown in Table 1.

Table 1. Literature review

Ref.	Morphological Parameter	Hemodynamic Parameter	Risk	Aneurysm	Diagnosis	Sensitivity	Accuracy	Method
[17]	Location	Blood flow velocity, Wall shear stress	Blood flow velocity >0.6 risk of aneurysm rupture					CFD
[26]	Location Size		Low, Medium, High	198	MRA	83		U-Net
[19]	Location Size	Comorbidity (Hypertension), History of hemorrhage, Ethnicity	European countries >3.6 *Finnish >2.8 *Japanese	230				PHASES
[27]	Location Size	Sex, Age, Comorbidity (Hypertension, Diabetes, Hyperlipidemia, Ischemic Cerebrovascular Disease), Smoking, Blood flow velocity, History of hemorrhage)		649		84		MAPN
[28]	Location Size	Age, Comorbidity (Hypertension, Epilepsy, Depression, Kidney disease), Smoking, History of hemorrhage, Ethnicity	Growth, Risk of rupture (Low-High)	277		80		UIATS
[1]	Location Size	Sex, Age, Wall shear stress, Blood flow velocity, Arterial pressure/Aneurysm neck, Ethnicity		226			78.1	Machine Learning (Random Forest)
[29]	Location Size	Sex, Age, Comorbidity, (Hypertension, Diabetes, Hyperlipidemia), Smoking, History of hemorrhage	Low, Medium, High	615		85		Machine Learning (SVM)
Our	Location Size Type	Sex, Age, Comorbidity (39 comorbidity are given in Table 2)	Percentage risk	253	CTA	93.75	81.8	Machine Learning (Neural Network)

The major risk for patients with cerebral aneurysms is rupture of the aneurysm and resulting fatal subarachnoid hemorrhage. Therefore, treatment should be initiated prior to any rupture that may occur in people with cerebral aneurysms.

The objective of the present study was to determine the risk of rupture as a percentage by examining the morphological structure and hemodynamic factors of all cerebral aneurysms, whether rupture or not. Accuracy is of critical importance when determining the risk status, as the possibility of rupture for existing aneurysms was evaluated using machine learning classification algorithms. For this purpose, a detailed data set that had not been used previously was created. This data set contains information on the width, length, location, and type of aneurysm, which constitute morphological characteristics. Additionally, patient-specific age, sex, and comorbidity parameters were included in the data set as they represent predictors affecting the risk of rupture. In order to increase the transparency of this study, the numerical and categorical data sets incorporating these seven predictors are presented in Appendix 1.

This study is comprised of three stages. First, an updated data set was created by examining the medical records of patients with cerebral aneurysms. In the second stage, classification was performed using machine learning algorithms for each morphological and hemodynamic parameter that may affect the risk of rupture in the aneurysm. Performance analysis results were obtained by analyzing the accuracy, specificity, precision, and sensitivity parameter values of the system. The final stage consisted of testing the trained classification network. For this purpose, the risk percentages of rupture in patients with cerebral aneurysms were determined using the external data set.

When evaluated in terms of innovation and contribution to scientific knowledge, our research can be considered to have yielded important results. In this section, we will present the innovations generated by our study. First, seven parameters, consisting of hemodynamic and morphological features, as well as rupture status for 39 different comorbidities were examined. To date, the impact of this variety of rupture status for different comorbidity parameters has not been examined in the literature. Since this situation directly affects the risk of rupture, it highlights a significant gap in the literature. Another innovation of our study involves the fact that heretofore no research has been conducted incorporating right-left and segment information regarding the location of the aneurysm; this represents yet another major deficiency in the literature. More importantly, in the present study aneurysms of all sizes were evaluated, without any exclusion criteria. As this also directly affects the risk of rupture, another gap in the literature is revealed. In addition to eliminating these deficiencies, the present study compared 23 different machine learning classification methods and determined rupture status using the Narrow Neural Network (NNN) classifier for the first time. In achieving this, for the first time, the risk of rupture could be expressed as a percentage. The disease histories of three patients with aneurysms were examined, and from the radiology reports rupture was determined to have occurred at later dates. With the machine learning classification performed in this study, the risk status expressed as a percentage was compared with the time at which rupture would occur for the first time in these three patients, and a 100% accurate result was obtained.

The present study contributes to the literature by providing guidance for neurosurgeons in determining the treatment

stages for patients with aneurysms. Furthermore, using NNN, a machine learning classifier algorithm, the rupture risk status was estimated for patients with aneurysms with a success rate of 81.8%. Additionally, in patients with saccular aneurysms, while the location of the MCA, a size of 2-10 mm, and the presence of heart disease and hypertension exerted major effects on the rupture status, other characteristics were observed to have a lesser effect.

2. DATA SET INFORMATION

The data set used in this study was obtained following approval from the Elazığ Firat University Ethics Committee. A random sample of recent and current (2011-2022) medical records of 220 patients diagnosed with cerebral aneurysms and suffering from subarachnoid hemorrhage was evaluated. A total of 93 ruptured and 127 unruptured aneurysms were detected in the 220 patients. Seven risk factors for the rupture of cerebral aneurysms were assessed in terms of their morphological and hemodynamic properties.

Registered patient data were obtained from the database of Firat University Hospital neurosurgery outpatient clinic follow-ups. A total of 220 patients with aneurysms were classified as ruptured or non-ruptured by three neurosurgeons with approximately 20 years of experience. Images of ruptured aneurysms taken from registered sample patients are shown in Figures 1(a) and (b), while an image of a non-ruptured aneurysm is depicted in Figure 1(c).

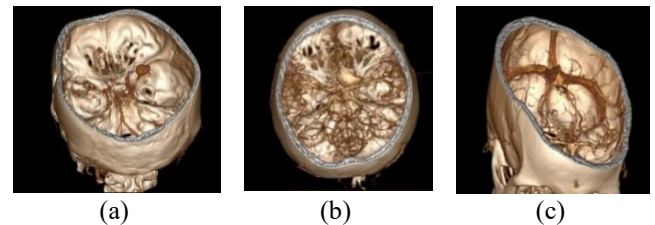


Figure 1. Data used for training: (a) and (b) ruptured aneurysms; (c) non-ruptured aneurysm

As an example, in Figure 1(a), a 15×12 mm ruptured saccular aneurysm was observed in the right MCA of a 61-year-old male patient with no comorbidities. Figure 1(b) shows the image of a 26×20 mm saccular ruptured aneurysm in the right ICA of a 68-year-old female patient with hypertension. Figure 1(c) depicts a 9.8×9.6 mm non-ruptured saccular aneurysm in the left ICA of a 44-year-old with ischemic cerebrovascular disease.

Documentation for the patient group represented in the data set includes morphological and hemodynamic characteristics. Morphological properties are defined as the characteristic features of an aneurysm, including its location, type, width, and length, whereas hemodynamic characteristics are specific to the patient and involve parameters such as age, sex, and comorbidities. Taking these features into account, the rupture (or non-rupture) statuses of an aneurysm for each parameter in the data set are presented in Table 2. The data for the age, width, and length parameters presented in the table represent average values.

A data set was created based on the medical records of 220 male and female patients with saccular and fusiform cerebral aneurysms, aged 22-94, in different locations and of various sizes. Among these patients, 93 had experienced ruptures

while 127 had not. In addition, 39 different comorbidities, evaluated in the data set, including hypertension, diabetes, goiter, and depression were

Table 2. Morphological and hemodynamic parameters of cerebral aneurysms

Parameter	Rupture (93)	Non-Ruptur (127)
Hemodynamic		
Age	62.05	62.04
Sex		
Female	57	78
Male	36	49
Comorbidity		
Diabetes	1	10
Depression	1	0
Goiter	1	0
Hypertension	22	21
Ischemic cerebrovascular disease	0	16
Cirrhosis	0	1
Restless leg	2	0
Ischemic heart disease	3	8
Hyperlipidemia	0	3
Chronic renal failure	3	0
Breast cancer	0	1
Coronary artery preparation	5	0
Heart failure	2	3
None	40	37
Lung cancer	0	2
Anxiety disorder	1	0
Atherosclerosis	0	1
Atrial fibrillation	0	1
History of embolism	1	0
Epilepsy	2	1
Essential hypertension	1	3
Gastritis	0	1
Gastroesophageal reflux	0	1
Pituitary adenoma	0	1
Chronic viral hepatitis	2	0
Bladder cancer	2	0
Multiple myeloma	1	0
Osteomyelitis	0	1
Parkinson's	2	0
Rheumatoid arthritis	0	2
Takayasu arteritis	0	2
Tremor	0	1
Trigeminal neuralgia	0	1
Vasculitis	0	1
Venous embolism	0	2
Kidney failure	0	1
Chronic ischemic heart disease	0	3
Chronic heart disease	1	1
Heart failure	0	1
Morphology		
Width	7.35	7.41
Length	6.44	6.51
Location		
AComA	22	25
ACA	7	11
Rigth	6	5
Left	1	6
ICA	19	32
Rigth	13	9
Left	6	23
MCA	28	49
Rigth	13	31
Left	15	18
Other (BA, PCA, VA)	17	10
Type		
Saccular	90	113
Fusiform	3	14

Note: Data are average values.

3. MATERIALS AND METHODS

In this study, a machine learning algorithm was modeled utilizing the morphological and hemodynamic characteristics of cerebral aneurysms. A data set was created by grouping the parameters for these features. These data were then applied as input to the neural network algorithm, a machine learning classifier, to determine the risk of rupture and non-rupture of cerebral aneurysms, referencing 220 cases with seven predictors. In instances of ruptured aneurysms, the connection with these features was examined and the importance emphasized. The architecture of the developed classification model proposed to determine the risk of rupture is shown in Figure 2.

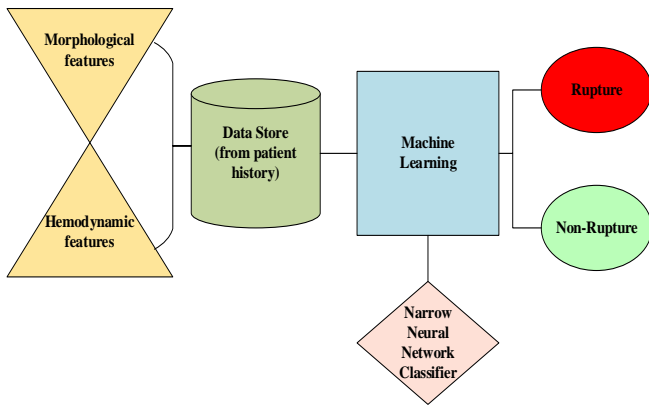


Figure 2. Machine learning classifier

The data set created in this study was applied as input to machine learning algorithms, with the desired output being the determination of the rupture status as a percentage. Since the neural network classification algorithm generated the best results in terms of accuracy during the classification process, it was used as a reference in the subsequent stages.

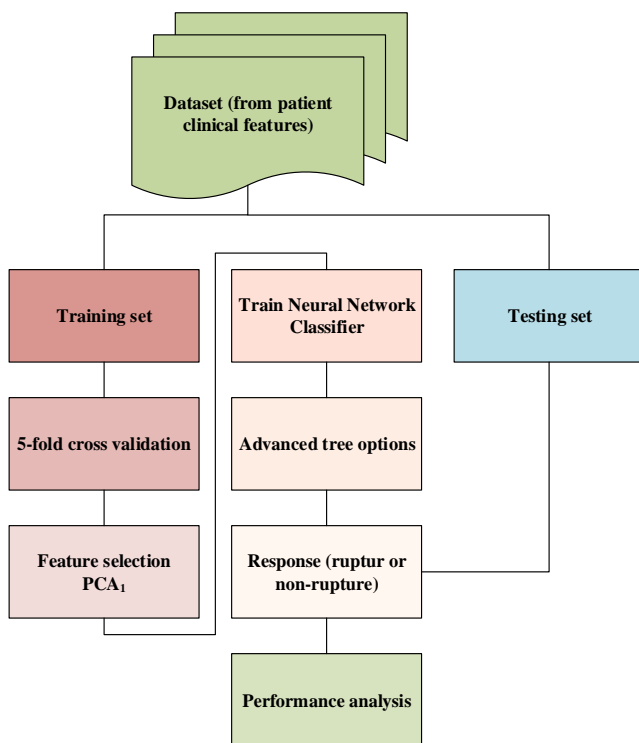


Figure 3. The proposed algorithm of the study

The neural network classifier is a proposed model-supervised machine learning algorithm. This algorithm was implemented with classifiers employed in the MatLAB R2023a classifiers application. These classifiers consist of decision trees, support vector machines, ensemble learning, logistic regression, and Bayesian classifier methods. In this study, the NNN classifier was used because its accuracy rate yielded the best results, while support vector machines are next in terms of high accuracy ranking. Neural network models are utilized for multi-class classification and enjoy high predictive accuracy, although difficult to interpret. As the size and number of fully connected layers in the neural network increase, the flexibility of the model increases. The MatLAB “fitcnet” function was employed in the training model for the neural network classifier. The highest accuracy for this data set was obtained with the NNN classifier. Additionally, the area under the Receiver Operator Characteristic curve (AU-ROC), accuracy, sensitivity, and specificity parameters were also included when conducting performance analysis for the machine learning classifiers. The machine learning algorithm used in this study is given in Figure 3.

3.1 NNN classification

The Narrow Neural Network classifier algorithm relies on a neural network structure with a limited number of layers and neurons. Compared to larger neural networks, narrow networks contain fewer parameters and are computationally lighter. This approach is ideal for small datasets or systems with limited computational resources. Unlike traditional deep learning models, it employs a narrow structure to reduce the number of parameters and mitigate issues like overfitting. This classifier algorithm accelerates data processing by providing a simpler and more efficient learning model. The Narrow Neural Network algorithm is preferred for its ability to quickly learn from limited datasets and perform satisfactorily in classification tasks. Additionally, they are generally preferred when the dataset is small or when there is a risk of model overfitting. However, it may be inadequate for complex and large data sets.

3.2 The operating of NNN

Input layer: The input layer receives features from the dataset.

Hidden layers: These networks consist of only a few layers (typically 1-2), each containing a limited number of neurons. Activation functions are applied within these layers to process the input data.

Output layer: As a classification problem, the output layer returns the predicted class. Activation functions such as softmax or sigmoid are typically used in this layer.

3.3 Mathematical models and parameters

The following general equations are used in narrow neural networks:

Weights and biases: Each neuron is associated with a weight (w) and a bias (b) that apply to the input features.

$$z = w \cdot x + b$$

where, x denotes the input data. The z value is then passed

through an activation function.

Activation functions: Activation functions such as ReLU or tanh are used in the hidden layers, while softmax or sigmoid functions are typically used in the output layer for classification tasks.

For example, a ReLU activation function is defined as:

$$f(z) = \max(0, z)$$

Loss function: To evaluate model performance, loss functions such as cross-entropy or mean squared error are applied. The loss function is critical in the backpropagation algorithm, where it facilitates updates to the weights and biases.

The model's optimization involved several key parameters: a learning rate of 0.1, which controlled the step size for weight updates during training, and a total of 30 learners, indicating the number of base models in the ensemble. Additionally, the estimator count was set to 7, defining the number of predictors used per estimation. A 5-fold cross-validation was conducted to enhance model generalizability and reduce overfitting risk by systematically partitioning the dataset for training and validation. Finally, the total misclassification cost was set to 160, imposing penalties on incorrect classifications to prioritize model accuracy. These parameters collectively contribute to balancing model accuracy, computational efficiency, and generalization.

4. EXPERIMENTAL FINDINGS

The NNN classifier, a supervised machine learning classification algorithm, was chosen for this study, based on the fact that this particular algorithm yields the highest accuracy rate during classification. With this method, hemodynamic and morphological parameters constitute the input to the network while rupture or non-rupture status forms the output. A split occurs for each node in the decision tree. Gini's diversity index was employed to ensure that the division occurred with zero error; the equation model for Gini's diversity index is given in Eq. (1).

$$1 - \sum_i p^2(i) \tag{1}$$

where the sum is over the classes i at the node, and $p(i)$ is the observed fraction of classes with class i that reach the node. A node with just one class (a pure node) has Gini index 0; otherwise, the Gini index is positive. So, the Gini index is a measure of node impurity.

High-performance GPU or CPU is a requirement for network training. For the present study, training was conducted using 16 GB RAM and an Intel Core i7 processor CPU. A data set consisting of the medical records of 220 cerebral aneurysm patients was used in the network training of the neural network algorithm, a machine learning classifier in the MatLAB programming language. In the training, the learning rate was 0.1, the number of learners was 30, the estimator count was 7, and a 5-fold cross-validation was performed. In addition, the total misclassification cost was 160, the prediction speed was 1800 obs/sec, and the training time was 3.38 sec. The model type was defined as NNN, the number of fully-connected layers was set at 1 and the first layer size was 10, with a Rectified Linear Unit (ReLU)

activation and an iteration limit of 1000. When selecting features, all characteristics were incorporated into the model prior to Principal Component Analysis (PCA₁). The training results consisted of binary output data: rupture or non-rupture. The location, type, and size of the aneurysms, along with the age, sex, and comorbidities of the patients were evaluated by neurosurgeons with approximately 20 years of experience, who determined the rupture status of the aneurysms. Their results were subsequently compared with those of the machine learning analysis.

In the experimental study, the medical records of 33 patients, 16 with ruptured and 17 with non-ruptured aneurysms, were used to perform external testing of the classification network. The trained network generated 27 correct and 6 incorrect predictions. While the trained network yielded an accuracy rate of 75%, the success of the study was further supported by the 81.8% accuracy calculated during the testing process. When the incorrectly detected data were evaluated, different parameters were observed for the seven predictors. Predictor variables that were not previously trained in the network were estimated incorrectly because they had been used in the testing process. The confusion matrix created during the testing process is shown in Figure 4.

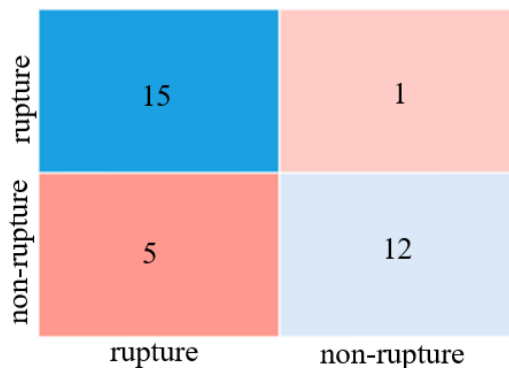


Figure 4. Test outcome confusion matrix

To evaluate the performance of the machine learning model, Accuracy (ACC), Sensitivity (SEN), Specificity (SPE), Precision (PRC), and F-score parameters were used as criteria for estimating the area under the Receiver Operating Characteristic (ROC) curve and aneurysm rupture risk. The equation models for these parameters are expressed as follows:

$$A_{CC} = \frac{tp + tn}{tp + tn + fp + fn} \tag{2}$$

$$S_{EN} = \frac{tn}{tn + fn} \quad S_{EN} = \frac{tp}{tp + fp} \tag{3}$$

$$S_{PE} = \frac{tp}{tp + fp} \quad S_{PE} = \frac{tn}{tn + fn} \tag{4}$$

$$P_{RC} = \frac{tn}{tn + fp} \quad P_{RC} = \frac{tp}{tp + fn} \tag{5}$$

$$F - score = \frac{2 * tp}{2 * tp + fp + fn} \tag{6}$$

where, true positive (tp), true negative (tn), false positive (fp), and false negative (fn) represent the coefficients of the confusion matrix.

Table 3. NNN classifier performance metrics

Machine Learning	Class	Sensitivity	Specificity	Precision	F-score	Accuracy (%)
Narrow Neural Network (NNN)	Rupture	0.613333	0.851485	0.754098	0.676471	75
	Non-rupture	0.851485	0.613333	0.747826	0.796296	
Testing process	Rupture	0.9375	0.705882	0.75	0.833333	81.8
	Non-rupture	0.705882	0.9375	0.923077	0.8	

Table 4. Data set created to predict rupture

Age	Width	Length	Location	Type	Sex	Comorbidity
59	8.5	5.5	LEFT MCA M2	Saccular	Male	None
45	7	8	RİGTH MCA M1	Saccular	Female	Hypertension
68	7	6	RİGTH MCA M2	Saccular	Female	None

Table 5. Classification results

Real	Rupture Condition	Prediction-Yes	Prediction-No
No	After 1 month	1	0
No	After 6 years	0.5920	0.4080
No	After 3 months	1	0

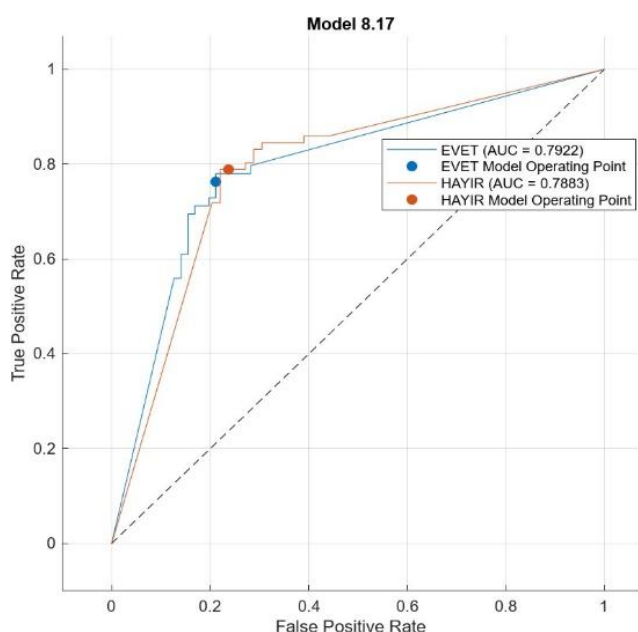


Figure 5. ROC curve

The ROC curve depicting the relationship between the true positive and false positive rates in the model is shown in Figure 5. The true positive rate used in the classifier is expressed as the positive prediction rate for “positive observation” while the false positive rate is expressed as the positive prediction rate for “negative observation”. The ROC curve is employed in conjunction with cross-validation to evaluate the model’s performance on test data. A 5-fold cross-validation was performed in this study. The performance metrics for the NNN classifier are shown in Table 3.

In the data set used for experimental purposes, prepared with regard to hemodynamic and morphological characteristics, subarachnoid hemorrhage was determined to have occurred at later dates in three patients with aneurysms who had not previously experienced rupture. Thus, for aneurysms not currently rupture, the risk of life-threatening subarachnoid hemorrhage will be mitigated by accelerating the treatment steps in the event of future rupture. In this study, rupture was predicted utilizing the proposed machine learning neural network classifier. Information from the patients’

radiology reports is presented in Table 4.

The rupture risk rates in the classification algorithms of three patients with aneurysms who experienced subsequent rupture are presented in Table 5 as a percentage.

Although there were no records of ruptures in the original radiology reports of the three patients, according to the NNN classifier model, the chance of ruptures occurring in these patients was predicted to be 100%, 59.2%, and 100%. Upon further examination of the patients’ disease histories, which included radiology results from later dates, their aneurysms were found to have ruptured after one month in the first patient, after 6 years in the second patient, and after 3 months in the third patient. According to hospital medical records, aneurysms were previously identified in three patients; however, these patients were not treated due to either patient preference or the inability to predict the likelihood of rupture. In the dataset, these three cases were identified, and their aneurysms ruptured after varying periods following the initial diagnosis. The NNN model was applied to test the seven parameters recorded at the time of the initial aneurysm diagnosis for these patients. The test results, detailing the risk percentages for the aneurysms, are presented in Table 5. Accordingly, two patients with a high-risk score (classified as 1) experienced ruptures 1 and 3 months after the initial diagnosis. In the third patient, whose risk score was 0.5920, a rupture occurred 6 months later.

5. RESULTS AND DISCUSSION

The data set used, incorporating the morphological and hemodynamic features obtained from the medical records of patients with ruptured and non-ruptured aneurysms, appears in Table 2. Raw data values for variable groups related to the various parameters are included in Appendix 1, while the graphic results generated by the training that affect rupture status are presented in Appendix 2. Accuracy rates and training times in determining rupture status for the different classification models are shown in Figure 6.

Among the 23 models that underwent training, the highest accuracy value, at 73.29%, was obtained with the neural network classifier, depicted as orange in the graph. In this decision tree, PCA1 was used to reduce the dimensionality of the prediction space. As a result, a new variable set was created by removing unnecessary dimensions. The model was developed by selecting features for the seven parameters determined in the study. The final result for the maximum accuracy rate of 75% in training is shown in purple in Figure 7, for model 17, which had a training time of 3.38 seconds.

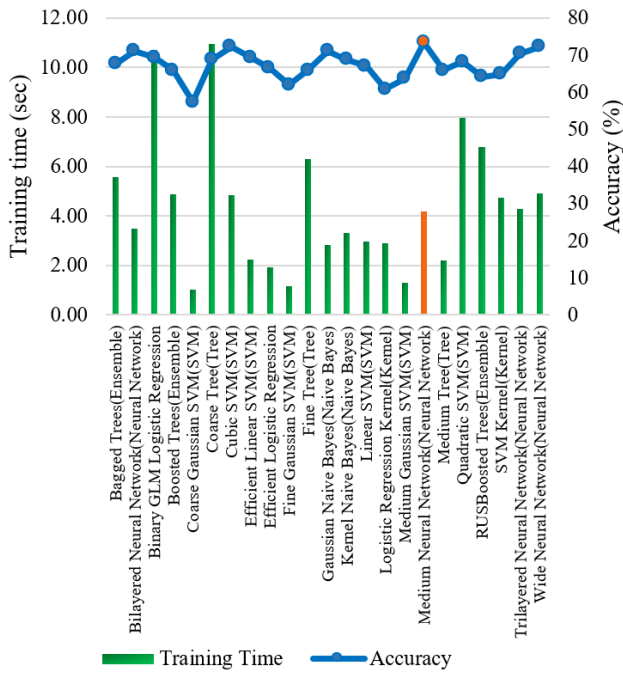


Figure 6. Training time and accuracy values of the different classification models

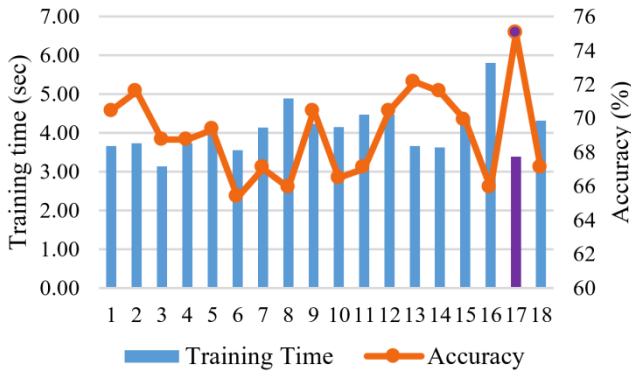


Figure 7. Training times and accuracy values for the proposed NNN classifiers

The improved NNN classifier used in this study, wherein morphological and hemodynamic features were considered in tandem, yielded the greatest accuracy with respect to rupture status. In this connection, training for the model was performed using the neural network classifier. The model results obtained for the NNN classifier, developed by applying PCA1, with the number of learners set to 30 and a learning rate of 0.1, are presented in Figure 8. Positive Predictive Value (PPV) represents the proportion of correctly classified observations for a given predicted class. Conversely, the False Discovery Rate (FDR) indicates the proportion of incorrectly classified observations within the predicted class. PPV is shown in blue for correctly predicted points in each class, while FDR is displayed in orange for incorrectly predicted points in each class. The relationship between PPV and FDR in model training is presented in Figure 8(b). The TPR (True Positive Rate) and FNR (False Negative Rate) metrics are fundamental measures used to evaluate a model's classification performance:

TPR (True Positive Rate): This is the rate at which positive instances are correctly classified as positive. Also known as "Sensitivity" or "Recall," this metric indicates the model's ability to identify true positive cases and is calculated as

follows:

$$TPR = TP / (TP + FN)$$

FNR (False Negative Rate): This represents the rate at which true positive instances are incorrectly classified as negative. This metric indicates the model's tendency to miss cases that belong to the positive class and is calculated as:

$$FNR = FN / (TP + FN)$$

Here,

TP (True Positive): The number of instances that are truly positive and correctly classified as positive by the model,

FN (False Negative): The number of instances that are truly positive but incorrectly classified as negative by the model.

TPR and FNR help evaluate the model's performance in correctly identifying positive class instances. High TPR and low FNR values indicate strong model performance in accurately recognizing instances belonging to the positive class. The relationship between TPR and FNR in model training is presented in Figure 8(a).

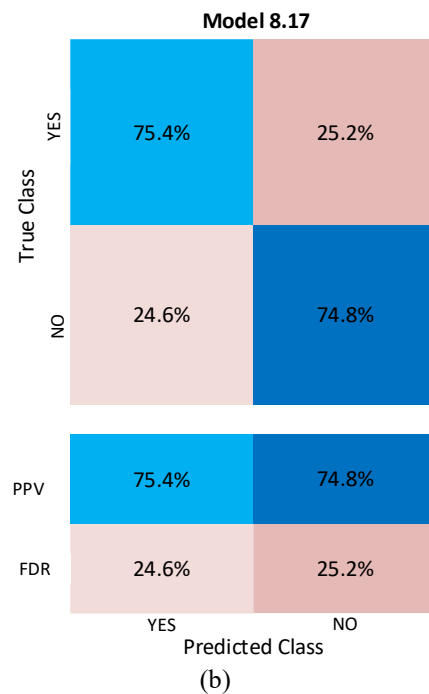
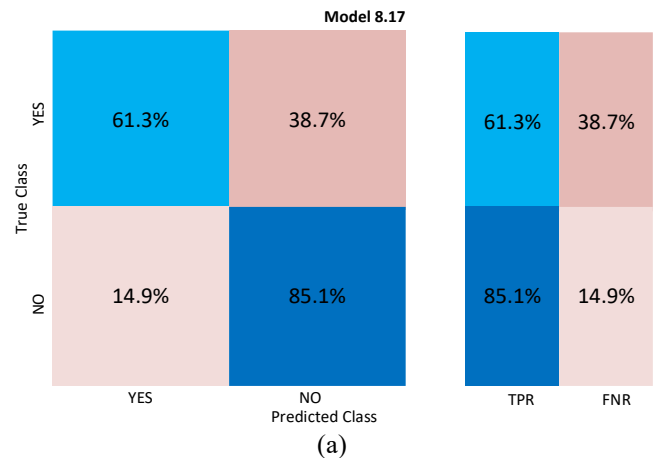


Figure 8. True positive-false negative rates of the NNN classifier

Here, the false negatives are shown in pink while true positives are depicted in blue. The highest accuracy value was calculated as 75%, with 46 true positives (*tp*) and 29 false positives (*fp*) for patient data indicating ruptures, and 86 true negatives (*tn*) and 15 false negatives (*fn*) for images without ruptures. The true positive rate (TPR) varied between 61.3%-85.1%, the false negative rate (FNR) ranged from 14.9%-38.7%, positive predictive values (PPV) were 75.4% and 74.8%, and false discovery rates (FDR) were calculated to be 24.6% and 25.2%.

Since rupture from cerebral aneurysms constitutes a major life-threatening risk, parameters that may cause rupture should be carefully considered. In this study, the classification of risk factors was performed incorporating such parameters. Graphs of the data on rupture in cerebral aneurysms for each risk factor are shown in Appendix 2. By applying the improved NNN classification algorithm, which yielded the best results in terms of accuracy, rupture was predicted to be detected in advance with an accuracy of 81.8% in the external testing process. This rate represents a level of accuracy that can prevent permanent damage and death in serious life-threatening illnesses. As a result of the machine learning classification process applied to the seven risk factors determined based on the medical records of patients diagnosed with cerebral aneurysms, rupture can now be predicted with great accuracy.

Ruptures, affected by morphological and hemodynamic parameters, induce subarachnoid hemorrhage. Such rupture can also occur in cases of head injury. Determining whether rupture is caused by an aneurysm or is a result of trauma presents difficulties. If rupture status can be established with high accuracy using machine learning, risky aneurysm surgeries can be avoided [1]. The machine learning classifier model employed in the present study incorporated the morphological and hemodynamic parameters of cerebral aneurysms in its analysis. Based on the resulting classification, the major risk factors triggering the rupture of saccular aneurysms were identified as MCA location and the comorbidities of heart disease and hypertension. Representing the estimated risk of rupture for cerebral aneurysms as a percentage demonstrates the applicability of this system, as do the relevant performance metrics obtained in this study.

In the future, the number of data points will be increased and information regarding the parameters of this data set will be expanded. With the use of different classification methodologies, it is anticipated that more general results can be obtained.

6. CONCLUSIONS

In this study, a highly accurate machine learning algorithm model was developed to assist neurosurgeons in determining the rupture risk of cerebral aneurysms. Rupture risk status was estimated using this improved classification algorithm utilizing a data set created by evaluating the medical records of patients with cerebral aneurysms. The training accuracy of the proposed model was 75%, the highest yielded accuracy. The classification results of the trained network exhibited a true positive rate of 85.1% and a false negative rate of 14.9% for patients who had experienced ruptures, with a positive predictive value of 75% and a false discovery rate of 24.6%. In patients whose aneurysms did not rupture, the true positive rate and false negative rates were 61.3% and 38.7%,

respectively. For such cases, a positive predictive value of 74.8% was calculated, with a false discovery rate of 25.2%. An external test set was prepared and the medical records of 33 patients were evaluated to test this improved network. A value of 81.8% was obtained for the validation accuracy of this classification resulting from the testing performed on this network. The close similarity in the values of the validation rates obtained in the training and test scenarios attests to the success of this study. This proposed model is anticipated to provide support for diagnosis and detection by examining the various risk factors for a wide variety of diseases. In the present study, the data of patients whose aneurysms had not previously ruptured but did rupture at subsequent follow-ups were collected. Patients who had not actually experienced rupture but whose data indicated future rupture also underwent follow-up. Based on the machine learning classifiers developed in this study, it was concluded that the aneurysms in these patients would eventually rupture. The probability of rupture in previously non-ruptured aneurysms can thus be calculated as a percentage, a result that is expected to have a guiding effect on the treatment of patients with cerebral aneurysms and to support neurosurgeons.

6.1 Limitations

Classification accuracy generally increases with an increase in the number of samples. In this context, the need to increase the number of patients for the optimal development of the model constitutes the main limitation of this study.

Another limitation is the fact that the data set used in this study included only the medical records of patients diagnosed with cerebral aneurysms. In order to detect other diseases and compare classification accuracy using machine learning, the risk factors of different diseases must also be considered.

Since the data used in this study were obtained from a single institution, data from different institutions should also be included, in order to generalize the classification. Additionally, data inaccuracies caused by human error when creating parameters represent an important variable impacting classification accuracy.

6.2 Future directions

The number of real patient records in the dataset will be increased.

The parameters WSS, velocity, OSI, and pressure are not currently included among the hemodynamic factors. These parameter values will also be incorporated into the dataset and evaluated in addition to the existing seven input variables.

Data from patients with different medical conditions will be collected, and more generalized results will be obtained using the applied classification methodologies.

ACKNOWLEDGMENT

The authors would like to thank Sait Öztürk, Bekir Akgün and Ahmet Cemil Ergün for their contributions to the data set.

REFERENCES

- [1] Tanioka, S., Ishida, F., Yamamoto, A., Shimizu, S., Sakaida, H., Toyoda, M., Kashiwagi, N., Suzuki, H.

- (2020). Machine learning classification of cerebral aneurysm rupture status with morphologic variables and hemodynamic parameters. *Radiology: Artificial Intelligence*, 2(1): e190077. <https://doi.org/10.1148/ryai.2019190077>
- [2] Urbizu, A., Martin, B.A., Moncho, D., Rovira, A., Poca, M.A., Sahuquillo, J., Macaya, A., Espanol, M.I. (2017). Machine learning applied to neuroimaging for diagnosis of adult classic Chiari malformation: Role of the Basion as a key morphometric indicator. *Journal of Neurosurgery*, 129(3): 779-791. <https://doi.org/10.3171/2017.3.JNS162479>
- [3] Kothapalli, P.K.V., Rathikarani, V., Nookala, G.K.M. (2022). Prediction of dyslexia and attention deficit and hyperactivity disorder prediction using ensemble classifier model. *International Journal of System Assurance Engineering and Management*. <https://doi.org/10.1007/s13198-022-01724-z>
- [4] Delucchi, M., Spinner, G.R., Scutari, M., Bijlenga, P., Morel, S., Friedrich, C.M., Furrer, R., Hirsch, S. (2022). Bayesian network analysis reveals the interplay of intracranial aneurysm rupture risk factors. *Computers in Biology and Medicine*, 147: 105740. <https://doi.org/10.1016/j.compbiomed.2022.105740>
- [5] Ley, C., Martin, R.K., Pareek, A., Groll, A., Seil, R., Tischer, T. (2022). Machine learning and conventional statistics: Making sense of the differences. *Knee Surgery, Sports Traumatology, Arthroscopy*, 30(3): 753-757. <https://doi.org/10.1007/s00167-022-06896-6>
- [6] Parlett-Pelleriti, C.M., Stevens, E., Dixon, D., Linstead, E.J. (2023). Applications of unsupervised machine learning in autism spectrum disorder research: A review. *Review Journal of Autism and Developmental Disorders*, 10(3): 406-421. <https://doi.org/10.1007/s40489-021-00299-y>
- [7] Lawton, M.T., Vates, G.E. (2017). Subarachnoid hemorrhage. *New England Journal of Medicine*, 377(3): 257-266. <https://doi.org/10.1056/NEJMcp1605827>
- [8] Etminan, N., Rinkel, G.J. (2016). Unruptured intracranial aneurysms: Development, rupture and preventive management. *Nature Reviews Neurology*, 12(12): 699-713. <https://doi.org/10.1038/nrneurol.2016.150>
- [9] Morita, A., Fujiwara, S., Hashi, K., Ohtsu, H., Kirino, T. (2005). Risk of rupture associated with intact cerebral aneurysms in the Japanese population: A systematic review of the literature from Japan. *Journal of neurosurgery*, 102(4): 601-606. <https://doi.org/10.3171/jns.2005.102.4.0601>
- [10] Thompson, B.G., Brown R.D., Amin-Hanjani, S., Broderick, J.P., et al. (2015). Guidelines for the management of patients with unruptured intracranial aneurysms: A guideline for healthcare professionals from the American Heart Association/American Stroke Association. *Stroke*, 46(8): 2368-2400. <https://doi.org/10.1161/STR.0000000000000070>
- [11] Liang, L., Liu, M., Martin, C., Elefteriades, J.A., Sun, W. (2017). A machine learning approach to investigate the relationship between shape features and numerically predicted risk of ascending aortic aneurysm. *Biomechanics and Modeling in Mechanobiology*, 16: 1519-1533. <https://doi.org/10.1007/s10237-017-0903-9>
- [12] Chang, P.D., Kuoy, E., Grinband, J., Weinberg, B.D., et al. (2018). Hybrid 3D/2D convolutional neural network for hemorrhage evaluation on head CT. *American Journal of Neuroradiology*, 39(9): 1609-1616. <https://doi.org/10.3174/ajnr.A5742>
- [13] Algra, A.M., Lindgren, A., Vergouwen, M.D., Greving, J.P., Van Der Schaaf, I.C., Van Doormaal, T.P., Rinkel, G.J. (2019). Procedural clinical complications, case-fatality risks, and risk factors in endovascular and neurosurgical treatment of unruptured intracranial aneurysms: A systematic review and meta-analysis. *JAMA Neurology*, 76(3): 282-293. <https://doi.org/10.1001/jamaneurol.2018.4165>
- [14] Lee, G.J., Eom, K.S., Lee, C., Kim, D.W., Kang, S.D. (2015). Rupture of very small intracranial aneurysms: Incidence and clinical characteristics. *Journal of Cerebrovascular and Endovascular Neurosurgery*, 17(3): 217-222. <https://doi.org/10.7461/jcen.2015.17.3.217>
- [15] Dai, X., Huang, L., Qian, Y., Xia, S., Chong, W., Liu, J.J., Di Leva, A., Hou, X.X., Ou, C.B. (2020). Deep learning for automated cerebral aneurysm detection on computed tomography images. *International Journal of Computer Assisted Radiology and Surgery*, 15: 715-723. <https://doi.org/10.1007/s11548-020-02121-2>
- [16] Shu, Z., Chen, S., Wang, W., Qiu, Y., Yu, Y., Lyu, N., Wang, C. (2022). Machine learning algorithms for rupture risk assessment of intracranial aneurysms: A diagnostic meta-analysis. *World Neurosurgery*, 165: e137-e147. <https://doi.org/10.1016/j.wneu.2022.05.117>
- [17] Rostamian, A., Fallah, K., Rostamiyan, Y., Alinejad, J. (2023). Application of computational fluid dynamics for detection of high risk region in middle cerebral artery (MCA) aneurysm. *International Journal of Modern Physics C*, 34(2): 2350019. <https://doi.org/10.1142/S0129183123500195>
- [18] Di Noto, T., Marie, G., Tourbier, S., Alemán-Gómez, Y., Esteban, O., Saliou, G., Cuadra, M.B., Hagmann, P., Richiardi, J. (2022). Weak labels for deep-learning-based detection of brain aneurysms from MR angiography scans. In *MIDL 2022 Conference Short*.
- [19] Greving, J.P., Wermer, M.J., Brown, R.D., Morita, A., Juvela, S., Yonekura, M. (2014). Development of the PHASES score for prediction of risk of rupture of intracranial aneurysms: A pooled analysis of six prospective cohort studies. *The Lancet Neurology*, 13(1): 59-66. [https://doi.org/10.1016/S1474-4422\(13\)70263-1](https://doi.org/10.1016/S1474-4422(13)70263-1)
- [20] Aakash Kumar, P., Nandhini, D., Amutha, S., Syed Ibrahim, S.P. (2023). Detection and identification of healthy and unhealthy sugarcane leaf using convolution neural network system. *Sādhanā*, 48(4): 251. <https://doi.org/10.1007/s12046-023-02309-7>
- [21] Raju, M., P.Gopi, V., Anitha, V.S., Sherawat, A. (2023). Early diagnosis of Alzheimer's disease using wavelet-pooling based deep convolutional neural network. *Sādhanā*, 48(3): 173. <https://doi.org/10.1007/s12046-023-02219-8>
- [22] Shimpi, J.K., Shanmugam, P. (2023). A hybrid diabetic retinopathy neural network model for early diabetic retinopathy detection and classification of fundus images. *Traitement du Signal*, 40(6): 2711-2722. <https://doi.org/10.18280/ts.400631>
- [23] Asokan, S., Seshadri, A. (2023). hierarchical spatial feature-CNN employing grad-CAM for enhanced segmentation and classification in Alzheimer's and parkinson's disease diagnosis via MRI. *Traitement du Signal*, 40(6): 2769-2778. <https://doi.org/10.18280/ts.400637>

[24] Xiang, J., Yu, J., Choi, H., Fox, J.M.D., Snyder, K.V., Levy, E.I., Siddiqui, A.H., Meng, H. (2015). Rupture Resemblance Score (RRS): Toward risk stratification of unruptured intracranial aneurysms using hemodynamic-morphological discriminants. *Journal of Neurointerventional Surgery*, 7(7): 490-495. <https://doi.org/10.1136/neurintsurg-2014-011218>

[25] Takao, H., Murayama, Y., Otsuka, S., Qian, Y., Mohamed, A., Masuda, S., Yamamoto, M., Abe, T. (2012). Hemodynamic differences between unruptured and ruptured intracranial aneurysms during observation. *Stroke*, 43(5): 1436-1439. <https://doi.org/10.1161/STROKEAHA.111.640995>

[26] Di Noto, T., Marie, G., Tourbier, S., Alemán-Gómez, Y., Esteban, O., Saliou, G., Cuadra, M.B., Hagmann, P., Richiardi, J. (2023). Towards automated brain aneurysm detection in TOF-MRA: Open data, weak labels, and anatomical knowledge. *Neuroinformatics*, 21(1): 21-34. <https://doi.org/10.1007/s12021-022-09597-0>

[27] Shen, J., Huang, K., Zhu, Y., Weng, Y.X., Xiao, F., Mungur, R., Wu, F., Pan, J.W., Zhan, R.Y. (2023). Mean arterial pressure-aneurysm neck ratio predicts the rupture risk of intracranial aneurysm by reflecting pressure at the dome. *Frontiers in Aging Neuroscience*, 15: 1082800. <https://doi.org/10.3389/fnagi.2023.1082800>

[28] Molenberg, R., Aalbers, M.W., Mazuri, A., Luijckx, G.J., Metzemaekers, J.D.M., Groen, R.J.M., Uyttenboogaart, M., van Dijk, J.M.C. (2021). The Unruptured Intracranial Aneurysm Treatment Score as a predictor of aneurysm growth or rupture. *European Journal of Neurology*, 28(3): 837-843. <https://doi.org/10.1111/ene.14636>

[29] Silva, M.A., Patel, J., Kavouridis, V., Gallerani, T., Beers, A., Chang, K., Hoebel, K.V., Brown, J., See, A.P., Gormley, W.B., Aziz-Sultan, M.A., Kalpathy-Cramer, J., Arnaout, O., Patel, N.J. (2019). Machine learning models can detect aneurysm rupture and identify clinical

features associated with rupture. *World Neurosurgery*, 131: e46-e51. <https://doi.org/10.1016/j.wneu.2019.06.231>

NOMENCLATURE

ACoM	Anterior Communicating Artery
ACA	Anterior Cerebral Artery
ICA	Interior Cerebral Artery
MCA	Middle Cerebral Artery
PCA	Posterior Cerebral Artery
BA	Basilar Artery
VA	Vertebral Artery
SAK	Subarachnoid Hemorrhage
CTA	Computerized Tomography Angiography
MRA	Magnetic Resonance Angiography
TOF-MRA	Time-of-Flight Magnetic Resonance Angiography
PHASES	Population, Hypertension, Age, Size, History of hemorrhage, Location
UIATS	Unruptured Intracranial Aneurysm Treatment Score
MAPN	Field Factor
CPU	Central Processing Unit
GPU	Graphics Processing Unit
ReLU	Rectified Linear Unit
AUC	Area Under the Curve
AUROC	Receiver Operator Characteristic Curve
TPR	True Positive Rate
FPR	False Positive Rate
FNR	False Negative Rate
PPV	Positive Predictive Value
FDR	False Discovery Rate
PCA1	Principal Component Analysis
CVD	Cerebrovascular Disease